SPECTRAL CHARACTERISTICS OF RECLAIMED VEGETATION IN A RARE EARTH MINE AND ANALYSIS OF ITS CORRELATION WITH THE CHLOROPHYLL CONTENT**

H. Li [1*], Zh. Wei [1], X. Wang [2], F. Xu [1]

[1] College of Architecture and Surveying Engineering,
Jiangxi University of Science and Technology,
Ganzhou Jiangxi 341000, China; e-mail: giskai@126.com
[2] College of Economic Management, Jiangxi University of Science and Technology,
Ganzhou Jiangxi 341000, China

Due to special mining technology, ionic rare earth mines easily change the surrounding surface soil properties and cause damage to the ecosystem, which leads to difficulties in vegetation ecological restoration. In this paper, tung trees, bamboo willow, and slash pine were selected as reclamation vegetation, and their spectral characteristics under ecological environmental stress were compared. In addition, by analyzing the correlation between their chlorophyll contents and spectral parameters, a theoretical basis for hyperspectral remote sensing for monitoring rare earth reclaimed vegetation growth is provided. The results show that the reflectance of the visible bands in the three vegetation types is less than 0.15, and there are different degrees of "redshifting" in the green peaks and red valleys; correlation analysis was carried out between the chlorophyll contents of the three vegetation types and the original spectra and derivative spectra. The optimal band in the original spectra was concentrated near the red valley. The first-order derivative spectra are more dispersed than the original spectra; the tung tree signal is concentrated in the red edge region, the slash pine signal is located in the near-infrared band, and the bamboo willow signal is located near the green peak and the red edge band. The three vegetation types have some of the same but also different chlorophyll-sensitive parameters. Among them, REP is the maximum parameter for the tung tree, D_r is the maximum parameter for slash pine, and $SD_r - SD_b/SD_b + SD_r$ is the maximum parameter for bamboo willow, which can provide a reference for the construction of inversion models of different vegetation chlorophyll contents.

Keywords: *reclaimed land of ionic rare earth mining area, chlorophyll content, spectral characteristic parameter, correlation analysis.*

СПЕКТРАЛЬНЫЕ ХАРАКТЕРИСТИКИ ВОССТАНОВЛЕННОЙ РАСТИТЕЛЬНОСТИ И АНАЛИЗ ИХ КОРРЕЛЯЦИИ С СОДЕРЖАНИЕМ ХЛОРОФИЛЛА НА ТЕРРИТОРИИ РУДНИКА ПО ДОБЫЧЕ РЕДКОЗЕМЕЛЬНЫХ МЕТАЛЛОВ

H. Li [1*], Zh. Wei [1], X. Wang [2], F. Xu [1]

УДК 581.5;547.979.7

[1] Колледж архитектуры и геодезии, Университет науки и техники Цзянси,
341000, Цзянси, Китай; e-mail: giskai@126.com
[2] Колледж экономического менеджмента, Университет науки и техники провинции Цзянси,
341000, Цзянси, Китай

(Поступила 21 января 2019)

Вследствие специальной технологии добычи разработка месторождений редкоземельных элементов изменяет свойства поверхности окружающей почвы и наносит ущерб экосистеме, что приводит к трудностям в экологическом восстановлении растительности. В качестве восстанавливаемой растительности выбраны тунговые деревья, бамбуковая ива и карибская сосна. Сопоставлены

** Full text is published in JAS V. 87, No. 3 (http://springer.com/journal/10812) and in electronic version of ZhPS V. 87, No. 3 (http://www.elibrary.ru/title_about.asp?id=7318; sales@elibrary.ru).

их спектральные характеристики в условиях экологического стресса окружающей среды. Путем анализа корреляции между содержанием в них хлорофилла и спектральными параметрами создана теоретическая основа гиперспектрального дистанционного зондирования для мониторинга восстановления растительности после воздействия редкоземельных элементов. Полученные результаты показывают, что коэффициент отражения в полосах видимого диапазона для трех типов растительности <0.15, а в пиках в зеленой области и провалах в красной наблюдаются различные степени "красного смещения". Проведен корреляционный анализ между содержанием хлорофилла в трех типах растительности и исходными спектрами и спектрами производных. Оптимальная полоса в исходных спектрах сосредоточена вблизи красного провала. Спектры производных первого порядка более дисперсны, чем исходные спектры; сигнал, соответствующий тунговому дереву, сосредоточен на красном крае области, сигнал карибской сосны расположен в ближнем инфракрасном диапазоне, а сигнал бамбуковой ивы находится вблизи зеленого пика и красного края полосы. Эти три типа растительности имеют несколько одинаковых и несколько различных параметров, чувствительных к хлорофиллу. Среди них REP — максимальный параметр для тунгового дерева, Dr — для карибской сосны, а SDr-SDb/SDb + SDr — для бамбуковой ивы, что может служить ориентиром для построения инверсионных моделей различного содержания хлорофилла в растительности.

Ключевые слова: *восстановленная почва в зоне добычи редкоземельных элементов, содержание хлорофилла, параметр спектральной характеристики, корреляционный анализ.*

Introduction. Ionic rare earth metals (REs) are mainly distributed in Jiangxi, Guangxi, Fujian and other regions in southern China, and they contain medium- and heavy-weight REs. The mining methods of REs include various processes such as pond leaching, heap leaching, and in situ leaching, resulting in environmental impacts during the mining process such as the destruction of surface soil and vegetation. Because the soil becomes infused with leaching liquid, mining easily causes desertification and pollution of the soil, making the natural restoration of vegetation difficult. Therefore, the mining area mainly relies on artificial planting for reclamation. However, soil degradation and potential heavy metal pollution in mining areas leads to poor vegetation growth. Therefore, it is important to monitor the ecological status of vegetation growth. As an indicator of vegetation stress and external disturbance, chlorophyll can provide insight into the nutritional status of vegetation. Therefore, the real-time and accurate estimation of chlorophyll content is very important for large-scale vegetation growth monitoring. Moreover, by calculating the correlation between vegetation spectral parameters and chlorophyll content, the highlighted sensitive parameters can lay a foundation for chlorophyll estimation.

Scholars have carried out many related research studies. For example, Lu Xia [1] found that there was a significant correlation at the red edge location and vegetation index by analyzing the correlation between chlorophyll content and canopy reflectance spectra of vegetation such as jing, Shan apricot, and mulberry trees in a mining area. Hou Huifang et al. [2] found that the spectral correlation of each vegetation type was different, which was determined between the chlorophyll content and the original spectra and between the chlorophyll content and the transformation spectra by studying humulus, corn, bitter vegetables, and tung trees in a gold mining area. Ming et al. [3] found that the logarithmic spectral curve was significantly correlated with chlorophyll by studying the correlation between the canopy spectrum and the chlorophyll content of soybeans, corn, and poplar in the Gunzhou mining area. By studying the chlorophyll content and spectral response of maize seedlings under different iron concentrations, Ma et al. [4] found that the spectral parameters with a significant correlation with chlorophyll at different concentrations were different. By studying many herbaceous plants, Cui et al. [5] found that the vegetation indices TCARI and OSAVI were significantly correlated with chlorophyll content. These studies show that both of the spectral characteristics of vegetation and ecological parameter responses are closely related to vegetation type, growth environment and degree of stress. The soil in a mining area is polluted by heavy metals due to the penetration of wastewater, which causes the chlorophyll content in growing vegetation to decrease after absorbing certain heavy metal ions [6]. Ionic REs adopts the leaching method. The leaching solution from mining also destroys the soil structure and brings heavy metal pollution, which affects the healthy growth of the vegetation in the mining area. Thus, studying the spectral characteristics of vegetation and the response of ecological parameters under environmental stress in mining areas can lay a foundation for large-scale vegetation growth monitoring. This study implemented the typical reclaimed vegetation of rare earth mining as the research focus. First, the spectral characteristics of vegetation under ecological stress were analyzed, which can provide a basis for monitoring the restoration of the ecological environment in rare earth mining areas. Then, the correlation of

spectral characteristic parameters and vegetation indexes with chlorophyll were evaluated, which can provide a theoretical basis for the construction of a chlorophyll content estimation model for reclaimed vegetation.

Data and methods. *Survey of the study area.* The Lingbei RE mine is located in northern Dingnan County, Jiangxi Province, which covers an area of approximately 200 km^2. Currently, this mine has been in operation for nearly 30 years, resulting in a large area of a sandy surface. Under such long-term RE mining, the pond leaching/heap leaching process accumulated a large number of mullock heaps and tailings. In addition, the leaching liquid destroyed the original soil structure and nutrient distribution, causing the ecological environment of the abandoned land to be destroyed, and the vegetation growth was poor. In this paper, the Aobeitang RE mine was selected as the study area, which is located south of Lingbei. The specific coordinates are 115°04'37″~115°05'41″E and 24°54'10″~24°56'42″N, and the area is approximately 1.5 km^2. This mine has experienced previous pool leaching/heap leaching and, later, in situ mining processes, leaving a large area of bare tailings. Since 2000, artificial reclamation has been gradually implemented. However, because of the serious soil desertification and the pollution of water resources, the growth of the vegetation is severely hindered. In this paper, bamboo willow, tung trees, and slash pine were selected as representative reclamation vegetation for hyperspectral study.

A field Spec4 spectrometer acquired from ASD was used to collect vegetation spectra. The spectral range was 350–2500 nm. The field spectral acquisition was in clear and cloudless weather in July 2017, while the leaves of the vegetation were in the mature stage. We chose an acquisition time between 12 a.m. and 2 p.m. and kept the probe vertically downward. Finally, white-board calibration was required before each measurement, and the measurement was completed within 1 minute of calibration. According to the principle of average distribution, 60 samples of each plant species were randomly measured in the study area. Each sample was measured 10 times, and the average value was selected as the reflection spectrum. When acquisition of each sample spectrum finished, the chlorophyll content was collected by a SPAD-502 chlorophyll instrument. In addition, the final chlorophyll content of the sample was determined as the average of 6 measurements distributed evenly on the sample.

Spectral noise processing. In the measured spectrum, there were abnormal signals because of the influence of the instrument itself and water vapor in the atmosphere. To improve the accuracy of spectral curve analysis, it was necessary to delete the noise bands in the spectral curve. In this study, the final selection was 350–1350 and 1450–1750 nm after removing the water vapor noise within 1350–1450, 1750–2000, and 2350–2500 nm and the instrument within 2000–2350 nm.

First derivative spectrophotometric method. The first derivative method can be implemented to obtain the spectral change rate curve from the original spectral transformation and to obtain more spectral characteristic parameters from the spectral analysis. At the same time, the first derivative operation can reduce the influence of external factors such as illumination and soil on spectral accuracy. The specific formula is as follows:

$$R'(\lambda_i) = \frac{d\left(R(\lambda_i)\right)}{d\lambda} = \frac{R(\lambda_{i+1}) - R(\lambda_{i-1})}{2\Delta\lambda}, \quad (1)$$

where λ_1 is the wavelength of each band, $R(\lambda_i)$ is the original spectral reflectance at λ_i, $R'(\lambda_i)$ is the first derivative reflectance at λ_i, and $\Delta\lambda$ is the interval between λ_{i-1} and λ_i.

Continuum removal method. After applying the continuum transform, the spectral curves can be compared on a unified baseline. In addition, this transform operation can further amplify the spectral absorption characteristics and facilitate feature analysis of the absorption bands [7]. The specific formulas are as follows:

$$CR_i = R_i/R_{wi}, \quad (2)$$

$$R_{wi} = R_q + k(\lambda_i - \lambda_q), \quad (3)$$

$$k = (R_z - R_q)/(\lambda_z - \lambda_q), \quad (4)$$

where CR_i represents the value of continuum removal when the wavelength is λ_i, and R_q, R_z, and R_i are the reflectance at the start, end, and at i absorption, respectively; and λ_q, λ_z, and λ_i are the wavelength at the start, end, and at i absorption, respectively.

Selection of spectral parameters and vegetation indexes. The spectral parameters were extracted after spectral transformation of the original spectra, including three-sided matrix parameters, green peaks, red valleys, absorption characteristic parameters, and the ratio calculation of specific parameters. In addition, the vegetation indexes were always used to reflect physical and chemical properties, such as vegetation coverage and chlorophyll content, because the vegetation had the characteristics of low reflectance in the red band and

high reflectance in the near infrared band. There are many studies on the spectral parameters and vegetation index of non-mining areas. For example, Shi Bingquan et al. [8] constructed a chlorophyll estimation model of a *Pinus tabulaeformis* forest based on a "three-sided parameters"; Pan Bei et al. [9] estimated the chlorophyll content of apple leaves using hyperspectral indexes. However, there are few parameters for selection to study the spectral characteristics of vegetation in mining areas. In this paper, hyperspectral analysis of reclaimed vegetation in RE mining areas was carried out using various spectral characteristics (band location characteristics, spectral absorption characteristics, etc.). The selected spectral parameters and vegetation index are listed in Tables 1 and 2.

TABLE 1. Spectral Parameter

Spectral parameter	Definition	Description	Reference
D_b	Blue edge amplitude	Maximum derivation over 490–530 nm	[8]
λ_b	Blue edge position	The wavelength at D_b	[8]
SD_b	Blue edge area	Spectral integration over 490–530 nm	[8]
D_y	Yellow edge amplitude	Maximum derivation over 560–640 nm	[8]
λ_y	Yellow edge position	The wavelength at D_y	[8]
SD_y	Yellow edge area	Spectral integration over 560–640 nm	[8]
D_r	Red edge amplitude	Maximum derivation over 680–760 nm	[8]
λD_r	Red edge position	The wavelength at D_r	[8]
SD_r	Red edge area	Spectral integration over 680–760 nm	[8]
R_g	Green Peak reflectance	Maximum of original spectrum over 510–560 nm	[10]
λ_g	Green Peak position	The wavelength at R_g	[10]
R_r	Red Valley reflectance	Minimum of original spectrum over 640–680 nm	[10]
λ_v	Red Valley position	The wavelength at R_r	[10]
W	Absorption width	$\lambda_2 - \lambda_1$	[7]
H	Absorption depth	$1 - R_r$	[7]
A	Absorption area	H*W/2	[7]
K	Absorption slope	$(R_2 - R_1)$/W	[7]
SAI	Absorption index	$[S^* R_1+(1–S)^* R_2]/ R_r$	[7]
S	Absorption symmetry	$(\lambda_2 - \lambda_p)$/W	[7]
SD_r/SD_b	/	The ratio of SD_r to SD_b	[10]
SD_r/SD_y	/	The ratio of SD_r to SD_y	[10]
R_g/R_r	/	The ratio of R_g to R_r	[10]
$SD_r - SD_b/SD_r + SD_b$	/	The ratio of $SD_r - SD_b$ to $SD_r + SD_b$	[10]
$SD_r - SD_y/SD_r + SD_y$	/	The ratio of $SD_r - SD_y$ to $SD_r + SD_y$	[10]
$R_g - R_r/R_g + R_r$	/	The ratio of $R_g - R_r$ to $R_g + R_r$	[10]

N o t e. λ_p is the wavelength of the valley; λ_1 and λ_2 are the wavelengths of the shoulders on both sides of the valley; R_1 and R_2 are the reflectance of the shoulders on both sides of the valley; and R_p is the reflectance at the wavelength of the valley.

TABLE 2. Vegetation Indexes

Vegetation parameter	Formula	Reference
RSVI (red edge stress vegetation index)	(R714-R752)/2-R733	[11]
RENDVI (red edge-normalized difference vegetation index)	(R780-R680)/(R780+R680)	[11]
DD (double difference index)	(R750-R720)–(R700-R670)	[12]
REP (modified red edge position index)	700+40*(((R670+R780)/2-R700))/(R740-R700)	[13]
SAVI (soil-adjusted vegetation index)	(1+0.16)* (R800-R670)/(R800+R670+0.16)	[14]
TVI (triangle vegetation index)	0.5*(120*(R750-R500)-200*(R670-R550))	[15]
mND705 (modified normalized difference	(R750-R705)–(R750+R705-2*R445)	[16]
mSR705 (modified ratio index)	(R750-R445)–(R705-R445)	[16]

N o t e. R_i is the reflectance at wavelength i.

Results and analysis. *Analysis of the original spectrum.* By comparing the original spectral curves of three kinds of reclaimed vegetation (Fig. 1), it was found that the spectral trends of the reclaimed vegetation were basically consistent with those of normal vegetation. In the visible light range (400–760 nm), the pigments in the vegetation spectrum strongly absorbed the incident light, and the reflectance was less than 0.15 overall. In addition, chlorophyll mainly absorbed blue light (450 nm) and red light (670 nm) but absorb less green light (550 nm) during photosynthesis. Thus, an absorption valley in the blue and red bands formed a distinct green peak in the green band. The spectral reflectance increased sharply in the 680–760 nm band, forming a typical "red edge" feature in the spectral curves of the vegetation. In addition, the spectral reflectance in the near-infrared region (760–1350 nm) was significantly higher than that in the visible range. Near 961 and 1200 nm, two absorption valleys were generated due to the effect of cell structures. The spectral reflectance in the mid-infrared band (1300–1750 nm) first increased and then decreased after removing the dominant band of water vapor. However, due to the influence of external stress factors, such as soil desertification and soil salinization, the reflectance and wavelength of the characteristic peaks and valleys change, as shown in Table 3.

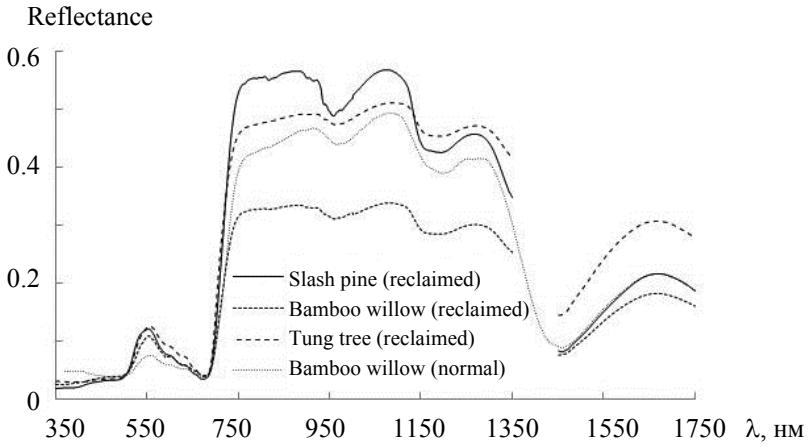

Fig. 1. The average original spectral curve.

Taking bamboo willow as an example, the spectrum of the mining area is compared with that of a normal bamboo willow spectrum. As shown in Fig. 1, it is clear that there was an obvious difference in the spectral curves. The "redshift" phenomenon seen in the vegetation in the mining area is further confirmed by data outlined in Table 4. The data show that the reflectance of reclaimed bamboo willow was higher than that of normal bamboo willow in both the green peak and the red valley. In terms of wavelength, the reclaimed bamboo exhibited spectral shifts to longer wavelengths of 3 nm for the green peak and 4 nm for the red valley.

TABLE 3. Reclaimed Vegetation Green Peak and Red Valley Reflectivity and Wavelength Position

Type	Green peak		Red valley	
	reflectance	wavelength	reflectance	wavelength
Slash pine	0.1205	553	0.0338	671
Bamboo willow	0.1091	555	0.0405	675
Tung tree	0.1256	556	0.0389	675

TABLE 4. Bamboo Willow Green Peak and Red Valley Reflectivity and Wavelength Position

Type	Green peak		Red valley	
	reflectance	wavelength	reflectance	wavelength
Normal bamboo willow	0.0759	552	0.0387	671
Reclaimed bamboo willow	0.1091	555	0.0405	675

First derivative spectral analysis. As shown in Fig. 2, the trend of the three vegetation spectral curves is generally consistent. At the same time, the derivative spectral curves were sharper, and the spectral characteristics that can be seen were more obvious. There are maximum points near 550, 778, 1050, 1270, and 1660 nm and minimum points near 665, 985, 1175, and 1450 nm. The low reflectance of the three types of vegetation within 350–450 nm led to little change in reflectance. However, a steep slope appeared from 450–550 nm and reached a maximum at 550 nm, mainly because of the absorption of blue and green light by chlorophyll. In addition, the typical "red edge" position in the 680–760 nm region caused the first-order spectral reflectance of the three types of vegetation to rise and fall sharply.

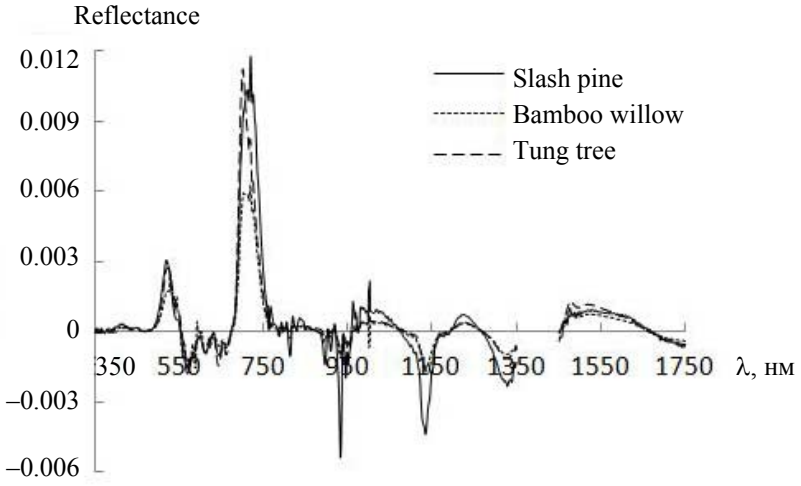

Fig. 2. The first derivative spectral curves.

To obtain the differences between the first derivative spectra of the three types of vegetation, the parameters of the "three-sided parameter matrix" were evaluated. The results are shown in Table 5. In terms of the blue-edge amplitude, the order from large to small is slash pine > tung tree > bamboo willow, while the position of the blue-edge amplitude is quite different. The values of D_y for the three types of vegetation were positive and negative, and the values for slash pine and tung tree were equal. For slash pine and tung tree, the λ_y increment was 1 nm. However, the increment value of $\mathbf{D}_y$ for bamboo willow differed from that of the other two vegetation types by 0.0005, and the λ_y value was much lower than that of the other two types. In the red-edge band, the D_r values of slash pine and tung tree were not much different, but the λ_r values differed by 18 nm, and there was a relatively obvious "blueshift." It should be noted that tung tree was more sensitive than the other vegetation types to the environmental impact of mining areas. Bamboo willow had a lower D_r value than other vegetation, and λ_r was close to that of slash pine.

TABLE 5. First-order Derivative Spectral Parameter Statistics

Type	D_b	λ_b	D_y	λ_y	D_r	λ_r
Slash pine	0.0031	519	-0.0001	630	0.0118	719
Bamboo willow	0.0025	529	0.0004	592	0.0063	719
Tung tree	0.0027	523	-0.0001	629	0.0112	701

Removal continuum spectral analysis. Comparing the absorption characteristics of different vegetation removal continuums, the results of the removal continuum are as follows. As shown in Fig. 3, the absorption and reflection characteristics of each band were more obvious. In this study, the red-edge absorption peak is compared as an example. The specific absorption spectrum parameters are shown in Table 6.

It is concluded that different vegetation types have distinct adaptations to the ecological environment. Therefore, their absorption capacities are different. As a parameter of absorption depth, the value of H reflects the absorption capacity of different vegetation types. SAI, as another expression of spectrum depth, had the same changes as H. In terms of absorption capacity, the order was slash pine > tung tree > bamboo

willow. In addition, the differences in absorption area and absorption slope of the three vegetation types were quite obvious, which can be used to distinguish the vegetation types. The differences in absorption symmetry were not obvious, mainly because the red valley position did not change much, and the right shoulder position of the three vegetation types was similar due to the presence of the red edge position.

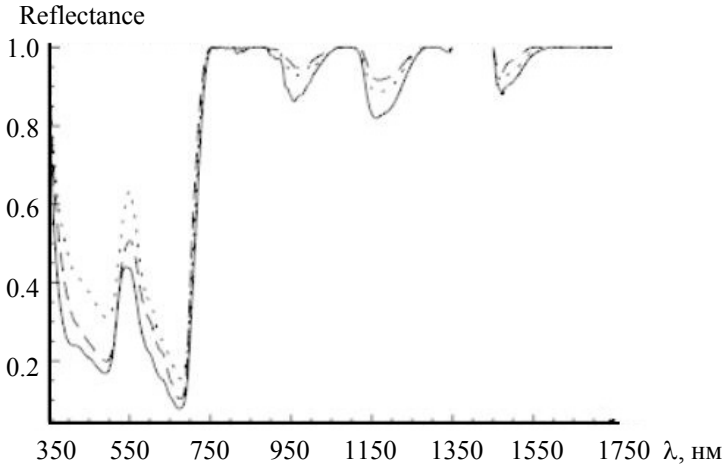

Fig. 3. Continuum removal spectral curve.

TABLE 6. Continuum Removal Spectral Parameter Statistics

Type	λ_p	R_p	W	H	A	K	SAI	S
Slash pine	674	0.0781	208	0.9219	95.8776	0.0023	10.2143	0.3606
Bamboo willow	677	0.1545	203	0.8455	85.8183	0.0018	5.5749	0.3793
Tung tree	676	0.1030	201	0.8970	90.1485	0.0045	7.8747	0.3831

Correlation analysis between chlorophyll content and spectral parameters and vegetation indexes. As an important physical and chemical parameter of vegetation, chlorophyll is often used for correlation analysis with spectral characteristics to lay a foundation for further establishing an estimation model of chlorophyll content. However, there were some differences in the spectral changes of the different vegetation types, resulting in an inconsistent selection of sensitive characteristic parameters when correlation analysis was performed. In this paper, the correlation analysis of the original spectrum, first derivative spectrum, and chlorophyll content of three reclamation vegetation types was carried out. The results are shown in Table 7. In the selection of sensitive bands, the wavelength of the maximum correlation coefficient is generally used as the selection parameter.

TABLE 7. Sensitive Band Selection

Spectrum	Tung tree		Slash pine		Bamboo willow	
Original	695 nm	–0.67**	684 nm	0.48*	699 nm	–0.49*
Derivative	666 nm	0.76**	921 nm	–0.48*	554 nm	–0.59**
	683 nm	–0.76**	877 nm	0.44*	742 nm	0.64**

* Represent significant correlation ($P < 0.05$);
* Represent extremely significant correlation ($P < 0.01$).

It was found that the positions of the sensitive band of the original spectrum were concentrated in the red edge region. However, the correlation coefficients were quite different, following the trend from large to small: tung tree > bamboo willow > slash pine. In addition, the tung tree spectral band was extremely signifycantly correlated with chlorophyll content, and bamboo willow and slash pine were significantly correlated with chlorophyll content. The correlation between the first-order derivative spectrum and the chlorophyll content is analyzed, and there are positive and negative correlations with the sensitive bands. The tung tree

and bamboo willow bands exhibited an extremely significant correlation, and the slash pine band exhibited a significant correlation with the chlorophyll content. In addition, the tung tree band was focused in the red-edge region, the slash pine band was focused in the shortwave infrared region, and the bamboo willow band was near the green peak and red-edge regions.

To further understand the correlation between chlorophyll content and spectral characteristics, correlation analysis was performed with the spectral parameters and the vegetation indexes (see Tables 1 and 2) as independent variables. The extraction results are based on the significant correlation, as shown in Table 8. The results in Table 8 reflect the similarities and differences in the selection of sensitive parameters for the different vegetation types.

TABLE 8. Sensitive Spectral Parameters and Vegetation Index Selection

	Bamboo willow		Slash pine		Tung tree	
Three-sided Matrix Parameters	D_b	–0.74**	D_b	0.5*	λ_b	0.81**
	SD_b	–0.7**	SD_b	0.4*	SD_b	–0.7**
	λ_b	0.82**	D_y	–0.5*	λ_g	–0.73**
	D_y	0.69**	SD_y	–0.5*	λ_v	–0.72**
	λ_y	–0.78**	D_r	0.77**	SD_r/SD_b	0.78**
	SD_y	0.68**	λ_r	–0.55**	$SD_r - SD_b/SD_r + SD_b$	0.82**
	D_r	–0.64**	D_r	0.79**	$SD_r - SD_y/SD_r + SD_y$	–0.69**
	λ_r	0.56**	R_g	0.45*	/	
	R_g	–0.74**	/		/	
	λ_g	0.61**	/		/	
	R_v	–0.62**	/		/	
	λ_v	–0.63**	/		/	
	SD_r/SD_b	0.82**	/		/	
	SD_r/SD_y	–0.77**	/		/	
	$SD_r - SD_b/SD_r + SD_b$	0.83**	/		/	
	$SD_r - SD_y/SD_r + SD_y$	–0.76**	/		/	
Absorption spectrum	S	0.84**	S	0.44*	S	0.51*
	H	0.43*	/		H	0.56**
	A	0.61**	/		A	0.63**
	K	0.69**	/		K	0.66**
	/	/	/		SAI	0.45*
Vegetation index	DD	0.8**	OSAVIVI	0.63**	DD	0.78**
	MND705	0.82**	TVI	0.73**	REP	0.83**
	MSR705	0.75**	RVSI	–0.76**	MND705	0.82**
	RENDVI	0.62**	/		MSR705	0.71**
	REP	0.82**	/		/	
	TVI	–0.64**	/		/	

* Represent significant correlation ($P < 0.05$);
* Represent extremely significant correlation ($P < 0.01$).

Correlation analysis was performed between the chlorophyll content and the three-sided matrix parameters as independent variables. Regarding tung tree, the correlation coefficients of the sensitive three-sided matrix parameters were all relatively large. The minimum correlation coefficient was 0.69 at $SD_r - SD_y/SD_r + SD_y$, the maximum was 0.82 at $SD_r - SD_b/SD_b + SD_r$, and the correlation coefficients of λ_b, λ_g, and λ_v were all greater than 0.7; the correlation coefficient of 0.81 at λ_b was close to the maximum observed coefficient. This result indicated that tung tree exhibited the band position as a sensitive parameter when extracting the three-sided matrix parameters. The correlation coefficients of the sensitive parameters of slash pine were low, with an average of approximately 0.5. However, the correlation coefficients at D_r and SD_r were very large, 0.77 and 0.79, respectively. The result indicated that it was easier to obtain satisfactory results by focusing on the red edge when the sensitive three-sided matrix parameters were extracted from

slash pine. For bamboo willow, the correlation was significant between chlorophyll content and almost all three-sided matrix parameters. In addition, the parameters with correlation coefficients above 0.8 were composed of blue and red bands. By correlating the absorption spectrum parameters and chlorophyll content, it was found that *S* was significantly correlated in all three vegetations. For slash pine, only *S* reached a significant correlation. For tung tree and bamboo willow, almost all parameters were significantly correlated. Among them, bamboo reached 0.84 for *S*.

The variation trend of the spectral curves of the different vegetation types was generally the same. However, there were differences in specific bands, reflecting the differences between species. The vegetation indexes were obtained by mathematical operations on the reflectance at specific bands. Therefore, it is reasonable that there are some differences in the vegetation index among different vegetation types. Comparing the statistical results, for tung tree, the vegetation indexes satisfying the correlation requirement is, from large to small, REP > MND705 > DD > MSR705 = 0.71; for slash pine, |RVSI| > |TVI| > |OSAVI| = 0.63; and for bamboo willow, MND705 = REP > DD > MSR705 > |TVI| > RENDVI = 0.62.

In this paper, the spectral characteristics of reclaimed vegetation in a RE mining area were analyzed by hyperspectral techniques. When the original spectrum of vegetation was studied, it was found that the spectral reflectance of the vegetation visible-light band was low. Moreover, the phenomenon of redshifting occurs at the green peak band and the red valley band. In previous studies, Y. Fang et al. [17] studied desert vegetation. It was found that the vegetation leaves were sparse and that the chlorophyll content was less under the influence of environmental stress than under normal growing conditions. At the same time, the spectral curve produced a “blue region redshift” phenomenon. This paper is consistent with Yang's research. However, the degree of “redshifting” was different; it is possible that different vegetation types have different degrees of response to ecological stress. In addition, many spectral characteristic parameters and vegetation indices were obtained after the first derivative and removal continuum transformations. Then, the correlation between each parameter and the chlorophyll content was calculated separately. The results showed that there were differences in the selection of sensitive parameters for the three kinds of reclaimed vegetation. In a study of chlorophyll content estimation based on red-edge parameters, Y. Fuqi et al. [18] found that the sensitive parameters of French paulownia and *Populus tomentosa* were different after a correlation analysis among the original spectrum, first derivative spectrum, red-edge parameter, and chlorophyll content. Therefore, the results of this paper are consistent with Yao's research. However, there are differences in the selection of the specific bands and sensitive parameters because of different vegetation types as the research focus. On the basis of certain achievements, this study should be further explored: the vegetation canopy is another important part of the plant, and its spectral variation should be further studied. In addition, spectral analysis should be carried out for each growth stage of the vegetation to determine the similarities and differences.

Conclusions. The spectral curves of the three reclaimed vegetation types had a blue valley near 450 nm, a red valley near 680 nm, and a green peak near 550 nm. Peak and valley characteristics were obvious. However, the spectral reflectivity increased rapidly in the 680–760 nm range, forming a red edge phenomenon. In addition, influenced by the absorption of vegetation pigments, the reflectance in the visible range was less than 0.15, which is consistent with the spectral characteristics of common vegetation.

Reclaimed vegetation in the mining area exhibited differences in wavelength and reflectance from the original spectral features of healthy vegetation. At the same time, there was a “redshift” phenomenon in the positions of the green peak and red valley. The reason for this shift is that the growth environment of reclaimed vegetation was poor, and the chlorophyll content of the vegetation decreased.

After the spectral curve was processed by first-order derivation and the removal continuum, there were many spectral characteristic parameters and vegetation indexes. All of them could be correlated with chlorophyll content. There were similarities and differences in the sensitive parameters of the three kinds of reclamation vegetation. The maximum correlation parameters of tung tree, slash pine and bamboo willow were REP = 0.83, D_r = 0.77, and $SD_r - SD_b/SD_b + SD_r$ = 0.83, respectively. The reason for this finding is that different vegetation types, due to their unique differences, form local differences in certain bands, even when the trend of the spectral curve is basically the same, and they have different responses to environmental impact factors in mining areas. The difference in the selection of sensitive parameters can provide a reference to construct inversion models of the chlorophyll contents of different vegetation types.

REFERENCES

1. L. Xia, *Geograph. Geo-Inform. Sci*., **26**, N 5, 37–40 (2010).
2. Hou Huifang, Qiao Xiaoying, Hao Ruijuan, Guo Yiwei, *J. Anhui Agric. Sci. Bull.*, **22**, N 11, 16–21 (2016).
3. Yanfang Ming, Lijuan Cheng, Huiyong Yu, Wang Chunxiang, *J. Ind. Soc. Remote Sens.*, **46**, N 1, 69–79 (2017).
4. Baodong Ma, Ao Xu, Xuanxuan Zhang, *IEEE Int. Geosci. Remote Sens. Symp. (IGARSS)* 10–15 (2016).
5. Shichao Cui, Kefa Zhou, *J. Earth Sci. Inform*., **10**, 169–181 (2016).
6. L. Xia, L. Shaofeng, Z. Liquan, *J. Sci. Surv. Mapping*, **32**, N 2, 111–113 (2007).
7. G. Chaofan, Xiaoyu Guo, *J. Acta Ecol. Sin.*, **36**, N 20, 6538–6546 (2016).
8. Shi Bingquan, Zhang Xiaoli, Bai Xueqi, Zhang Xinxin, *J. Northeast Forestry Univ.*, **43**, N 5, 80–83 (2015).
9. P. Bei, Z. Gengxing, Z. Xicun, Liu Haiteng, Liang Shuang, Tian Dade, *J. Spectrosc. Spectr. Anal*., **33**, N 8, 2203–2206 (2013).
10. L. Qingsan, W. Chuanyi, T. Xiaolei, Xu Jialai, Yang Jutian, Liu Li, Zhu Xianzhi, Zhang Yuqin, Xu Xiuhong, *Southwest China J. Agric. Sci*., **32**, N 2, 333–338 (2017).
11. D. Huaqiang, G. Hongli, F. Wenyi, Jin Wei, Zhou Yufeng, Li Jin, *J. Spectrosc. Spectr. Anal*., **29**, N 11, 30–37 (2009).
12. G. L. Maire, C. François, E. Dufrêne, *J. Remote Sens. Environ*., **89**, N 1, 1–28 (2004).
13. M. A. Cho, A. K. Skidmore, *J. Remote Sens. Environ*., **101**, N 2, 181–193 (2006).
14. G. Rondeaux, M. Steven, F. Baret, *J. Remote Sens. Environ*., **55**, N 2, 95–107 (1996).
15. N. H. Broge, E. Leblanc, *J. Remote Sens. Environ*., **76**, N 2, 156–172 (2001).
16. D. A. Sims, J. A. Gamon, *J. Remote Sens. Environ*., **81**, N 2-3, 337–354 (2002).
17. Y. Fang, C. Donghua, L. Hu, Li Jiangui, Xu Limin, *J. Remote Sens. Inform*., **31**, N 3, 88–93 (2016).
18. Yao Fuqi, Zhang Zhenhua, Yang Runya, Sun Jinwei, Cui Sufang, *J. Trans. CSAE*, **25**, N 2, 123–129 (2009).